

Nodal $d + id$ pairing and topological phases on the triangular lattice: unconventional superconducting state of $\text{Na}_x\text{CoO}_2 \cdot y\text{H}_2\text{O}$

Sen Zhou^{1,2} and Ziqiang Wang¹

¹*Department of Physics, Boston College, Chestnut Hill, MA 02467 and*

²*National High Magnetic Field Laboratory, Florida State University, Tallahassee, FL 32310*

(Dated: February 9, 2022)

We show that finite angular momentum pairing chiral superconductors on the triangular lattice have point zeroes in the complex gap function. A topological quantum phase transition takes place through a nodal superconducting state at a specific carrier density x_c where the normal state Fermi surface crosses the isolated zeros. For spin singlet pairing, we show that the second nearest neighbor $d + id$ -wave pairing can be the dominant pairing channel. The gapless critical state at $x_c \simeq 0.25$ has six Dirac points and is topologically nontrivial with a T^3 spin relaxation rate below T_c . This picture provides a possible explanation for the unconventional superconducting state of $\text{Na}_x\text{CoO}_2 \cdot y\text{H}_2\text{O}$. Analyzing a pairing model with strong correlation using the Gutzwiller projection and symmetry arguments, we study these topological phases and phase transitions as a function of Na doping.

PACS numbers: 74.20.-z, 74.20.Rp, 74.70.-b

The sodium cobaltate Na_xCoO_2 , a layered triangular lattice electron system, has received widespread interest since the recent discovery of the 5K superconducting (SC) phase in water intercalated $\text{Na}_x\text{CoO}_2 \cdot y\text{H}_2\text{O}$ near $x = 0.3$ [1]. While a very rich phase diagram is emerging for a broad range of Na concentrations [2], the nature of the superconducting phase has remained poorly understood. The main evidence that the SC phase is unconventional comes from the absence of the coherence peak in the in-plane NMR spin-lattice relaxation rate at T_c and its power law temperature dependence (T^3) below T_c [3, 4, 5]. Despite this evidence for an anisotropic SC gap function with line nodes, consistent with the specific heat [6] and μSR [7] measurements, there has been considerable debate over the pairing symmetry. Measurements of angle-averaged Knight shift in powdered samples have produced inconsistent results supporting either spin-triplet [8] or spin-singlet pairing [9]. The most recent measurements on high quality single crystals [10] show that the spin contributions to the Knight shift decreases below T_c along both the a and c -axis, which strongly supports that the Cooper pairs are formed in the spin-singlet state. The Knight shift and the relaxation rate above T_c show antiferromagnetic (AF) correlations [5, 10].

On the theoretical side, there has been a growing number of proposals for unconventional superconductivity in the cobaltates. For spin-singlet pairing in a non-s-wave channel, the six-fold symmetry of the triangular lattice requires the low angular momentum paired state to have the chiral $d_{x^2-y^2} \pm id_{xy}$ symmetry, raising the exciting possibility of a time-reversal symmetry breaking superconductor. Earlier studies that drew analogy to the high- T_c cuprates indeed found unanimously spin-singlet, $d + id$ pairing via the nearest neighbor AF superexchange in the triangular lattice t - J model at low doping [11, 12, 13, 14]. However, it is conventional wisdom that a $d + id$ paired state, as well as other chiral SC states with complex or-

der parameters, has a full gap and is thus inconsistent with NMR experiments [3, 4, 5].

In this paper, we show that extended chiral paired states beyond the nearest neighbor (NN) have generic point zeroes in the complex gap function *inside* the first Brillouin zone. Consider (ℓ, n) -wave pairing with angular momentum ℓ for the pairs on the n -th NN bond, the order parameter can be written down in real space,

$$\Delta_{ij} = \Delta_{\ell n} e^{i\ell\theta_{ij}}, \quad (1)$$

where ℓ labels the angular momentum of the pair and θ_{ij} is the angle of $\vec{r}_{ij} = \vec{r}_i - \vec{r}_j$ between sites i and j . The Fourier transform of Δ_{ij} is given by $\Delta_{\ell n}(k) = 2[\beta'_{\ell n}(k) + i\beta''_{\ell n}(k)]$, where the real (β') and the imaginary (β'') parts of the gap function are given in Table I in terms of the triangular lattice harmonics for the chiral p -wave ($\ell = 1$) and d -wave ($\ell = 2$) pairing. Nodes in the complex gap function arise where the real and imaginary parts of $\Delta_{\ell n}(k)$ vanish simultaneously, *i.e.* at the crossing points of the lines of zeroes of $\beta'(k)$ and $\beta''(k)$. Fig. 1 shows the locations of the gap nodes in the first zone for chiral p and d -wave pairing. For first NN pairing, the nodes are pinned to the zone center and zone boundary and thus a generic chiral $(\ell, 1)$ -wave superconducting state has a full gap. Remarkably, for the case of $n > 1$, new nodes in the gap function appear *inside* the zone and can support nodal $(\ell, n > 1)$ -wave superconducting states.

Hereafter we focus on the spin-singlet $d + id$ -wave case, *i.e.* chiral $(2, n)$ -paired states and argue that the existence of the nodes is relevant for understanding the superconducting state in hydrated cobaltates. For the second NN pairing with $n = 2$, there are six nodes inside the first zone marked by the solid circles in Fig. 1b. They are located at $\pm \mathbf{k}_\alpha^*$, with $\alpha = 1, 2, 3$, and $\mathbf{k}_1^* = 2\pi[2/(3\sqrt{3}), 0]$, $\mathbf{k}_2^* = 2\pi[1/(3\sqrt{3}), 1/3]$, and $\mathbf{k}_3^* = 2\pi[1/(3\sqrt{3}), -1/3]$, coinciding with the six corners of the hexagonal $\sqrt{3} \times \sqrt{3}$ reduced zone boundary.

Chiral p -wave pairing ($\ell = 1$):		
n	$\beta'_{1,n}(k)$	$\beta''_{1,n}(k)$
1	$\sqrt{3} \sin \frac{\sqrt{3}}{2} k_x \cos \frac{1}{2} k_y$	$\sin k_y + \cos \frac{\sqrt{3}}{2} k_x \sin \frac{1}{2} k_y$
2	$-\sqrt{3} \sin \frac{3}{2} k_y \cos \frac{\sqrt{3}}{2} k_x$	$\sin \sqrt{3} k_x + \cos \frac{3}{2} k_y \sin \frac{\sqrt{3}}{2} k_x$
3	$\sqrt{3} \sin \sqrt{3} k_x \cos k_y$	$\sin 2k_y + \cos \sqrt{3} k_x \sin k_y$

Chiral d -wave pairing ($\ell = 2$):		
n	$\beta'_{2,n}(k)$	$\beta''_{2,n}(k)$
1	$\cos k_y - \cos \frac{\sqrt{3}}{2} k_x \cos \frac{1}{2} k_y$	$\sqrt{3} \sin \frac{\sqrt{3}}{2} k_x \sin \frac{1}{2} k_y$
2	$\cos \sqrt{3} k_x - \cos \frac{3}{2} k_y \cos \frac{\sqrt{3}}{2} k_x$	$-\sqrt{3} \sin \frac{3}{2} k_y \sin \frac{\sqrt{3}}{2} k_x$
3	$\cos 2k_y - \cos \sqrt{3} k_x \cos k_y$	$\sqrt{3} \sin \sqrt{3} k_x \sin k_y$

TABLE I: Gap function $\Delta_{\ell n}(k) = 2[\beta'_{\ell n}(k) + i\beta''_{\ell n}(k)]$.

The first indication that this is special for the triangular lattice cobaltates comes from the fact that a single hexagonal Fermi surface (FS) at the SC concentration $x = 1/3$ matches the $\sqrt{3} \times \sqrt{3}$ reduced zone boundary such that these nodes would lie directly on the FS. Recent angle-resolved photoemission (ARPES) experiments in the both the unhydrated [15, 16] and the hydrated [17] compounds near $x \sim 0.3$ indeed observe a single rounded hexagonal FS that coincides well with the hexagonal $\sqrt{3} \times \sqrt{3}$ reduced k zone boundary. This is highly unexpected since the Co^{4+} has 5 d -electrons occupying the three t_{2g} orbitals. It turns out that strong correlation effects beyond the band theory renormalize the crystal field splitting and bandwidths, leading to a single quasiparticle band crossing the Fermi level as observed by ARPES experiments [18]. In Fig. 1b, we show the FS calculated in Ref. [18] at $x_c = 0.25$, which passes through the six gap nodes for the second NN $d + id$ -wave pairing. The value of x_c is smaller than $1/3$ due to the rounding of the hexagonal FS in both the ARPES data [15] and the theoretical calculations [18]. Interestingly, third NN $d + id$ -wave pairing introduces six nodes (Fig. 1b) at the corners of the hexagonal 2×2 reduced zone, which intersects the FS at $x = 1/2$ where the cobaltate is in an insulating phase with charge and spin order [2, 19].

The second, direct evidence for nodal $d + id$ -wave pairing at $x = x_c$ comes from the most recent NMR experiments. In high quality single crystals, Zheng *et al.* discovered that the T^3 decay of the relaxation rate $1/T_1$, *i.e.* the signature of line nodes in the gap function, is obeyed down to the lowest temperatures only at $x_c \simeq 0.26$, whereas deviations from T^3 are observed on both sides of x_c [5]. The existence of the Dirac nodes in the gap function at the critical doping x_c for spin-singlet pairing on the triangular lattice strongly favors the scenario of second NN $d + id$ -wave pairing. In the following, we report a variational study of the $(2, n)$ -wave pairing states in an effective single-band $t-U$ plus pairing model of the cobaltates, calculate the Knight shift and the spin relaxation rate $1/T_1$, and describe the topological prop-

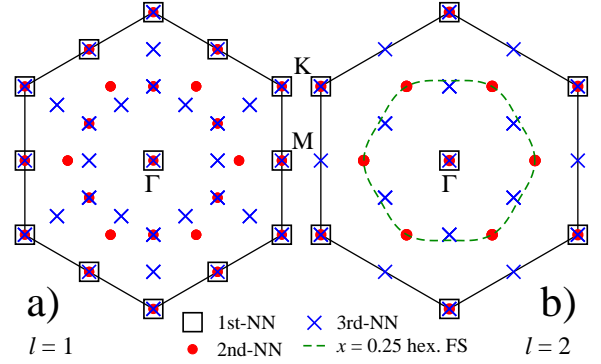


FIG. 1: Nodes of chiral (ℓ, n) -wave pairing where the gap function $\Delta_{\ell, n}(k)$ vanishes. (a) p -wave and (b) d -wave with normal state FS at $x = 0.25$ (dashed line).

erties of the superconducting phases.

The Hamiltonian is given on a triangular lattice,

$$H = \sum_{ij, \sigma} t_{ij} c_{i\sigma}^\dagger c_{j\sigma} + U \sum_i \hat{n}_{i\uparrow} \hat{n}_{i\downarrow} - \sum_{i,j} W_{ij} \hat{\Delta}_{ij}^\dagger \hat{\Delta}_{ij}, \quad (2)$$

where $c_{i\sigma}^\dagger$ creates a hole of spin σ and U is the Co on-site Coulomb repulsion. To describe the a_{1g} band crossing the Fermi level, we fix the first three NN hopping $t_{ij} = (t_1, t_2, t_3) = (-202, 35, 29)$ meV [19]. The hole density $n_i = 1 - x_i$ where x_i is the electron doping concentration. The last term in Eq. (2) is a phenomenological singlet pairing interaction $W_{ij} > 0$ between n -th NN sites i and j with $\hat{\Delta}_{ij} = c_{i\uparrow} c_{j\downarrow} - c_{i\downarrow} c_{j\uparrow}$. The effects of strong correlation are accounted for in the Gutzwiller approximation [20], leading to a renormalized band dispersion,

$$\begin{aligned} \xi_k = & 2g_t t_1 (\cos k_y + 2 \cos \sqrt{3} k_x / 2 \cos k_y / 2) \\ & + 2g_t t_2 (\cos \sqrt{3} k_x + 2 \cos \sqrt{3} k_x / 2 \cos 3k_y / 2) \\ & + 2g_t t_3 (\cos 2k_y + 2 \cos \sqrt{3} k_x \cos k_y) - \mu, \end{aligned} \quad (3)$$

where $g_t = 2x/(1+x)$ is the Gutzwiller renormalization factor in the large- U limit [19, 20]. The BCS state for $(2, n)$ -wave pairing can be written equivalently as [24]

$$|\Psi_n\rangle = \prod_k |u_{nk}|^{1/2} \exp\left(\frac{1}{2} g_{nk} c_{k\uparrow}^\dagger c_{-k\downarrow}^\dagger\right) |0\rangle, \quad (4)$$

where $g_{nk} = v_{nk}/u_{nk} = -(E_{nk} - \xi_k)/\Delta_{nk}^*$ and the quasiparticle excitation energy $E_{nk} = \sqrt{\xi_k^2 + |\Delta_{nk}|^2}$. The gap function is $\Delta_{nk} = 2W_n \Delta_n [\beta'_{2,n}(k) + i\beta''_{2,n}(k)]$, with β given in Table I. We first study the variational ground state obtained by minimizing the energy with respect to the only variational parameter Δ_n for a given W_n . In Fig. 2a, we compare Δ_n for the 1st, 2nd, and 3rd NN pairing with identical pairing strength $W_{1,2,3} = 50$ meV at several dopings. The 2nd NN $d + id$ pairing is the strongest with the largest pairing order parameter. Including a NN Coulomb repulsion V [21] would further suppress the 1st NN pairing attraction W_1 , making the

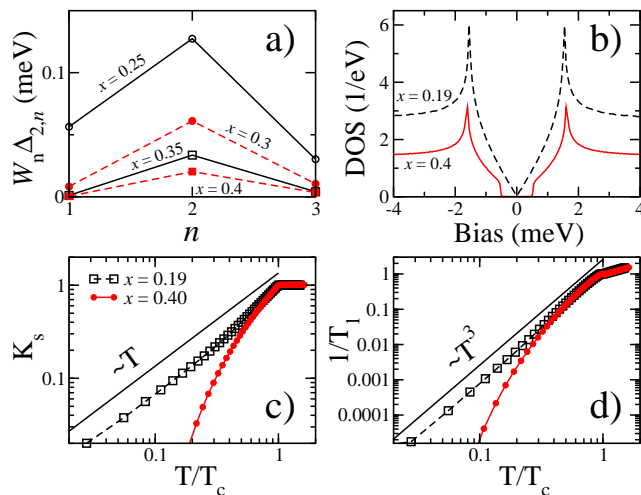


FIG. 2: (a) Comparison of $d+id$ pairing order parameters at several dopings for $W_{1,2,3} = 50$ meV. (b-d) Properties of 2nd NN $d+id$ -wave pairing at $x = 0.19 = x_c$ for $W_2 = 50$ meV and $x = 0.4 > x_c$ for $W_2 = 73$ meV: Tunneling DOS (b), temperature dependence of Knight shift K_s (c) and NMR relaxation rate $1/T_1$ (d) normalized by their values at T_c .

2nd NN $d+id$ -wave the dominant spin-singlet pairing channel that drives the SC transition. We emphasize that while the subdominant channels can emerge below the transition, the admixture of a small component with $n \neq 2$ would only result in small shifts of the six-fold symmetric point nodes in the gap function and not change the results discussed here.

Next we turn to the properties of the second NN $d+id$ state. For our band parameters, the FS is almost circular and $x_c \simeq 0.19$. At $x = x_c$, the normal state FS crosses the six nodes at $\pm \mathbf{k}_\alpha^*$ around which the quasi-particle dispersion E_k (hereafter we drop the index n) has a conical spectrum. For example, expanding around $\pm \mathbf{k}_1^*$, $E_k \simeq \sqrt{(A^2 + B^2)[k_x \mp 4\pi/(3\sqrt{3})]^2 + B^2 k_y^2}$, with $A = 3(t_1 - 2t_3)$ and $B = 9W\Delta/2$. Thus, the six nodes are described by three pairs of Dirac fermion doublets with anisotropic velocities. They govern the properties of the low energy excitations. We calculate the tunneling density of states (DOS) $N(E)$ and the temperature dependence of the ab -plane Knight shift (K_s) and the spin relaxation rate ($1/T_1$) according to

$$\left\{ K_s, \frac{1}{T_1} \right\} \propto - \int_{-\infty}^{\infty} \{1, TN(E)\} N(E) \frac{\partial f(E)}{\partial E} dE. \quad (5)$$

The results are plotted in Figs. 2b-d. The calculated $N(E)$ shows a linearly vanishing, V-shaped DOS at $x = x_c$ generic of nodal d -wave pairing. As a consequence, the Knight K_s and $1/T_1$ follow the T and T^3 behaviors below T_c in agreement with the NMR experiments on single crystals at $x \simeq 0.26$ [5, 10]. For $x \neq x_c$, the normal state FS does not overlap the nodes in the gap function. Fig. 2b shows that at $x = 0.4$ the DOS is fully

gapped at low energies, but reverts back to the V-shape above the energy gap. This leads to a rapid crossover of K_s and $1/T_1$ from the power law behaviors just below T_c to exponential decays at low temperatures (Figs. 2c and 2d). In this case, we expect that disorder-induced filling of the DOS gap to produce crossovers to constant K_s and linearly vanishing $1/T_1$ at low temperatures [3].

We now discuss the topological properties of the chiral SC states and the topological quantum phase transition as the carrier density x moves across x_c . The topological order in chiral fermion-paired states has been a subject of growing interests in connection to unconventional superconductors/superfluids and fractional quantum Hall states [22, 23, 24]. The key point is that the complex order parameter Δ_k and the dispersion ξ_k form a unit pseudospin vector introduced by Anderson [25]: $\mathbf{m}(k) = (\text{Re}\Delta_k, -\text{Im}\Delta_k, \xi_k)/E_k$. Since $|\mathbf{m}|^2 = 1$, \mathbf{m} lives on a 2-sphere S^2 . The SC state can be viewed as a BCS mapping from the \mathbf{k} -space, which is a torus T^2 (compactified from an infinite plane) to the pseudospin S^2 . This becomes evident when we write \mathbf{m} in term of the pairing function $g_k = v_k/u_k$ in Eq. (4),

$$m_1(k) + im_2(k) = -\frac{2g_k}{1 + |g_k|^2}, \quad m_3(k) = \frac{1 - |g_k|^2}{1 + |g_k|^2}. \quad (6)$$

Such maps are classified by homotopy classes with topological winding numbers Q . The lattice version of Q is,

$$Q = \frac{1}{8\pi} \sum_{\Delta} \mathbf{m}(k_1) \cdot [\mathbf{m}(k_2) \times \mathbf{m}(k_3)], \quad (7)$$

where the sum is over all elemental triangular plaquettes with corners labeled as 1, 2, 3. Topologically distinct phases are categorized by different winding numbers Q that count the number of times the pseudospin configuration \mathbf{m} wraps around the sphere. We find that $Q \neq 0$ if g_k has a *singular* vortex structure near the nodes of the complex gap function, a condition that depends on the location of the FS. In Fig. 3, we show the calculated Q for $x > x_c$, $x < x_c$, and at the critical state $x = x_c$. All of them are topologically nontrivial. For $x > x_c$, the normal state FS encloses only the gap node at the zone center where $g_k \propto 1/(k_x - ik_y)^2$, exhibiting a singular double vortex. This charge-two magnetic monopole contributes two flux quanta to the surface integral and gives $Q = \mp 2$ (Fig. 3) for the fully gapped topological phase. The sign corresponds to the relative sign of the real and imaginary parts of the order parameter. Note that near the nodes *outside* the FS, g_k behaves as zeroes, e.g. $g_k \propto k_x \mp 4\pi/(3\sqrt{3}) + ik_y$ near $\pm \mathbf{k}_1^*$, and thus do not contribute to Q . As the doping is reduced to $x < x_c$, the normal state FS encloses, in addition to the node at Γ , the six nodes at $\pm \mathbf{k}_\alpha^*$ where g_k exhibits singular vortex structure; e.g. $g_k \propto 1/[k_x \mp 4\pi/(3\sqrt{3}) + ik_y]$ near $\pm \mathbf{k}_1^*$. Each pair of the nodes can be viewed as a singular double vortex. The contribution to the magnetic flux through

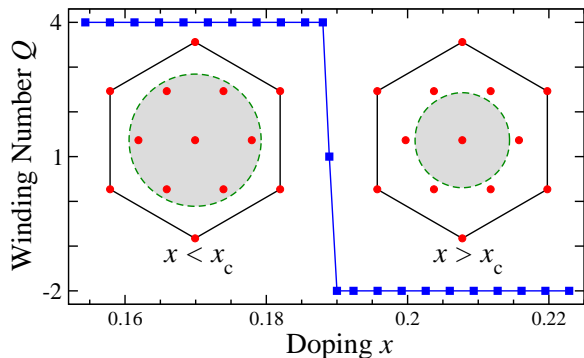


FIG. 3: Topological winding number as a function of doping in the second NN $d + id$ -wave superconducting state. Insets show the locations of the nodes in the complex gap function and the normal state FS.

the sphere is thus increased by six flux quanta leading to $Q = \pm 4$ as shown in Fig. 3.

In the critical state at $x = x_c$, the FS passes through the six gap nodes. The pseudospin vector \mathbf{m} is not well defined exactly at these isolated diabolic points, which are lattice-regulated in the summation in Eq. (7). Remarkably, Fig. 3 shows that the winding number $Q = \pm 1$ and the critical state is a gapless topologically nontrivial state. This suggests that each pair of the gap nodes in the critical state contributes a single vortex in k -space, reminiscent of the situation in the $p + ip$ state [24, 26]. Indeed, evaluating Q in the continuum limit along the line integrals of the six circles cutting out the nodes at \mathbf{k}_α^* , one finds that each of the latter contributes half a magnetic flux leading to the total $Q = \pm 1$. We note that the existence of such a *gapless* topological phase in two dimensions is new and consistent with the view point that gapless fermions emerge as a result of a form of quantum order [27] in the critical state. Physically, the topologically invariant winding number Q corresponds to the quantization of the spin Hall conductance σ_{xy}^s [23, 24]. In unit of the spin conductance quantum $(\hbar/2)^2/2\pi\hbar$, the spin Hall conductance is $\sigma_{xy}^s = Q$. Thus, we predict that as the electron doping x evolves across x_c , the superconducting state of the cobaltate exhibits quantum spin Hall transitions from ∓ 2 to ± 4 with quantized critical spin Hall conductance ± 1 . We expect novel properties associated with the edge states.

In summary, we have proposed a class of nodal chiral superconductors. The spin-singlet, second NN $d + id$ -wave pairing turns out to be consistent with the NMR experiments on high quality single crystals of hydrated cobaltate superconductors, and has some remarkable topological properties related to the quantum spin Hall transitions. Although the microscopic origin for the second NN $d + id$ pairing is beyond our scope here, it is conceivable that (i) a strong NN Coulomb repulsion [21], (ii) a larger 2nd NN superexchange, and (iii) the frustration of the NN antiferromagnetic correlation on the

triangular lattice and the proximity to inhomogeneous charge/spin ordered state [19, 21] will favor a dominant extended pairing interaction beyond the first NN. It is noted that the chiral pairing state breaks time-reversal symmetry which should in principle be detectable by μ SR or optical Kerr experiments with sufficient resolution. The orbital current near a unitary impurity produces a static magnetic field. To estimate the size of the field, we performed self-consistent calculations for the circulating current near a unitary impurity. The maximum current around the impurity site is ~ 100 nA for a pairing strength $W_2 = 50$ meV corresponding to a $T_c \sim 5$ K. This gives an estimate of the magnetic field at the impurity site ~ 1 G, which is close to the upper bound set by the earlier μ SR experiments [28, 29]. Future experiments are very desirable to determine whether time-reversal symmetry is broken in the superconducting cobaltates.

We are grateful to Y. Yu for many useful discussions. This work was supported by DOE grant DE-FG02-99ER45747 and NSF grant DMR-0704545.

-
- [1] K. Takada, *et al.*, Nature (London) **422**, 53 (2003).
 - [2] M. L. Foo, *et al.*, Phys. Rev. Lett. **92**, 247001 (2004).
 - [3] T. Fujimoto, *et al.*, Phys. Rev. Lett. **92**, 047004 (2004).
 - [4] K. Ishida, *et al.*, J. Phys. Soc. Jpn, **72**, 3041 (2003).
 - [5] G.-q. Zheng, *et al.*, J. Phys.: Condens. Matter **18**, L63 (2006).
 - [6] H. D. Yang, *et al.*, Phys. Rev. B **71**, 020504 (2005).
 - [7] A. Kanigel, *et al.*, Phys. Rev. Lett. **92**, 257007 (2004).
 - [8] M. Kato, *et al.*, J. Phys.: Condens. Matter **18**, 669 (2006).
 - [9] Y. Kobayashi, *et al.*, J. Phys. Soc. Jpn. **74**, 1800 (2005).
 - [10] G.-q. Zheng, *et al.*, Phys. Rev. B **73**, 180503 (2006).
 - [11] G. Baskaran, Phys. Rev. Lett. **91**, 097003 (2003).
 - [12] B. Kumar and B. S. Shastry, Phys. Rev. B **68**, 104508 (2003).
 - [13] M. Ogata, J. Phys. Soc. Jpn. **72**, 1839 (2003).
 - [14] Q.-H Wang, D.-H Lee, and P. A. Lee, Phys. Rev. B **69**, 092504 (2004).
 - [15] H.-B. Yang, *et al.*, Phys. Rev. Lett. **95**, 146401 (2005); Phys. Rev. Lett. **92**, 246403 (2004).
 - [16] M. Z. Hasan, *et al.*, Phys. Rev. Lett. **92**, 246402 (2004).
 - [17] T. Shimojima, *et al.*, Phys. Rev. Lett. **97**, 267003 (2006).
 - [18] S. Zhou, *et al.*, Phys. Rev. Lett. **94**, 206401 (2005).
 - [19] S. Zhou and Z. Wang, Phys. Rev. Lett. **98**, 226402 (2007).
 - [20] D. Vallhardt, Rev. Mod. Phys. **56**, 99 (1984); F.C. Zhang, *et al.* Supercond. Sci. Technol. **1**, 36 (1988).
 - [21] O. I. Motrunich and P. A. Lee, Phys. Rev. B **69**, 214516 (2004); **70**, 024514 (2004).
 - [22] G.E. Volovik, JETP Lett. **66**, 522 (1997).
 - [23] T. Senthil, J.B. Marston, and M.P.A. Fisher, Phys. Rev. B **60**, 4245 (1999).
 - [24] N. Read and D. Green, Phys. Rev. B **61**, 10267 (2000).
 - [25] P.W. Anderson, Phys. Rev. **110**, 827; **112**, 1900 (1958).
 - [26] G.E. Volovik, Sov. Phys. JETP **67**, 1804 (1988).
 - [27] X. G. Wen and A. Zee, Phys. Rev. B **66**, 235110 (2002).
 - [28] W. Higemoto, *et al.*, Phys. Rev. B **70**, 134508 (2004).
 - [29] Y. J. Uemura, *et al.*, arXiv:cond-mat/0403031 (2004).